Electronic Supplementary Material (ESI) for Journal of Materials Chemistry A.
This journal is © The Royal Society of Chemistry 2023

Supporting Information

Core-Shell InN/PM6 Z-scheme Heterojunction Photoanodes for Efficient and Stable Photoelectrochemical Water Splitting

Shaohua Xie,[a,b] Jiehui Liang,[a,b,c] Qianhu Liu,[a,b,c] Peixin Liu,[a,b] Junkun Wang,[a,b,c] Jiaxi Li,[a,b] Haoyang Wu,[a,b] Wenliang Wang [a,b,*] and Guoqiang Li [a,b,c,d,*]

[a] State Key Laboratory of Luminescent Materials and Devices, South China University of Technology, Guangzhou 510640, China.

[b] Department of Electronic Materials, School of Materials Science and Engineering, South China University of Technology, Guangzhou 510640, China.

[c] School of Physics and Optoelectronics, South China University of Technology, Guangzhou 510640, China.

[d] Guangdong Choicore Optoelectronics Co., Ltd., Heyuan 517003, China

[*] Corresponding author, E-mail: wenliangwang@scut.edu.cn and msgli@scut.edu.cn

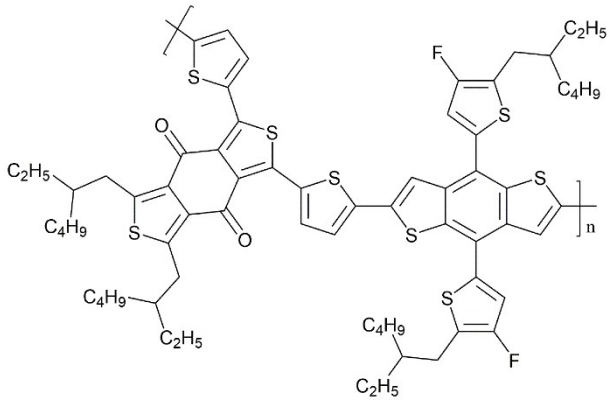

Fig. S1. Chemical structures of PM6.

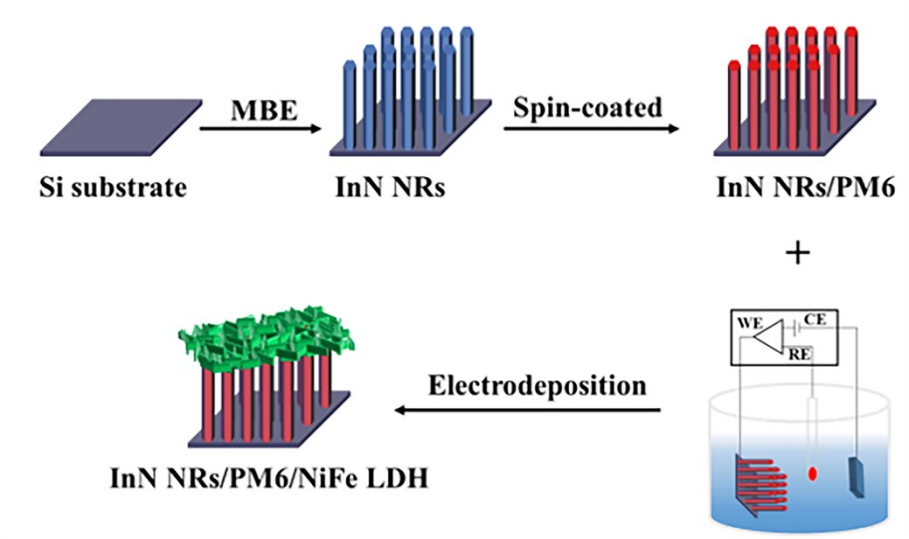

Fig. S2. Schematic diagram for the preparation of the InN/PM6/NiFe LDH photoelectrode.

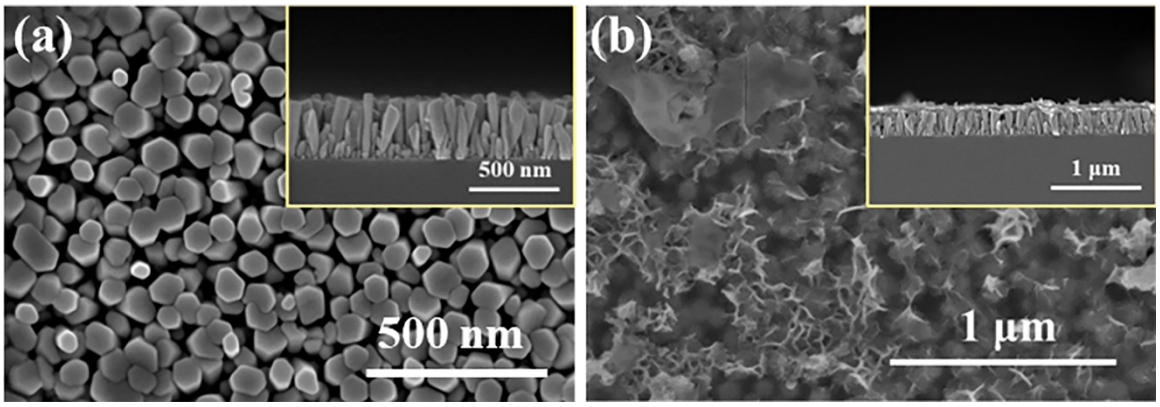

Fig. S3. The top view of SEM image of (a) InN NRs and (b) InN/PM6/NiFe LDH photoelectrode. The inset is the corresponding side view of SEM image.

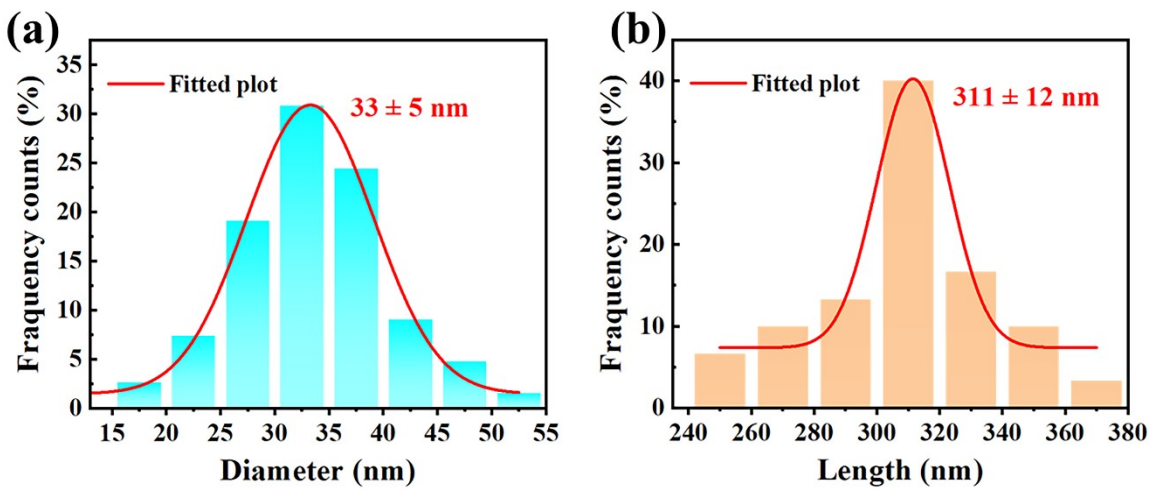

Fig. S4. The diameter (a) and length distribution (b) of the InN NRs.

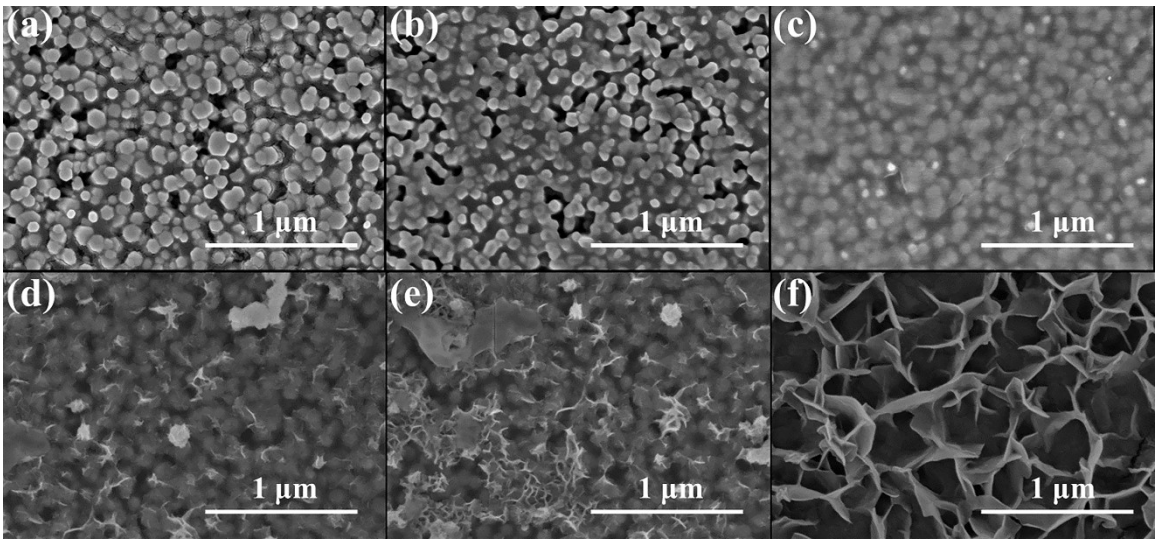

Fig. S5. (a-c) The top-view SEM images of InN/PM6-3000, InN/PM6-4000, and InN/PM6-5000. (d-f) The top-view SEM images of InN/PM6/NiFe LDH-60, InN/PM6/NiFe LDH-120, and InN/PM6/NiFe LDH-180.

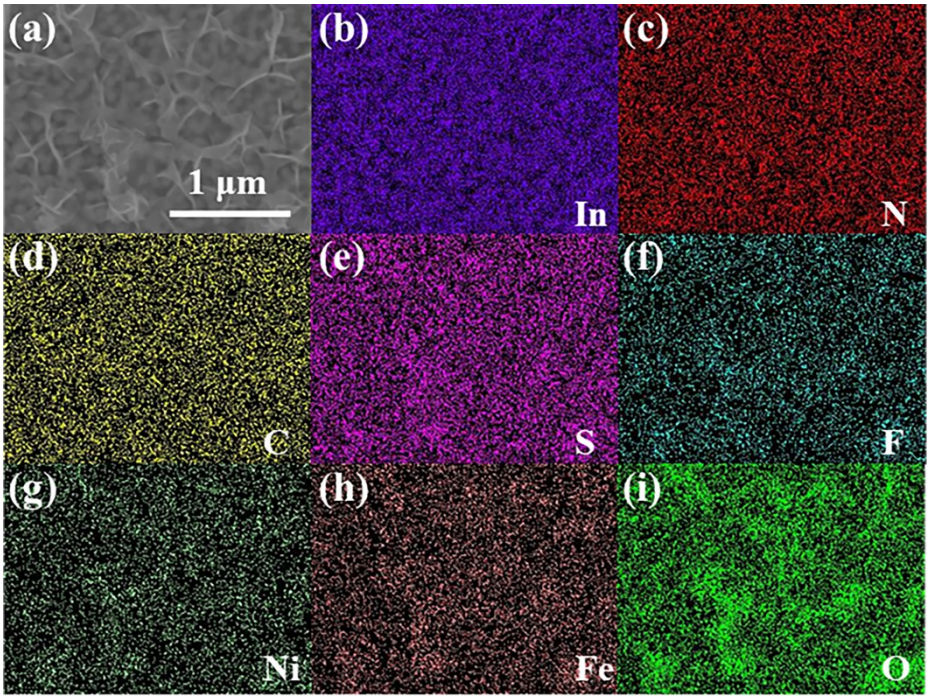

Fig. S6. (a) SEM top view images and (b-i) the corresponding elemental mapping images of the InN/PM6/NiFe LDH photoelectrode.

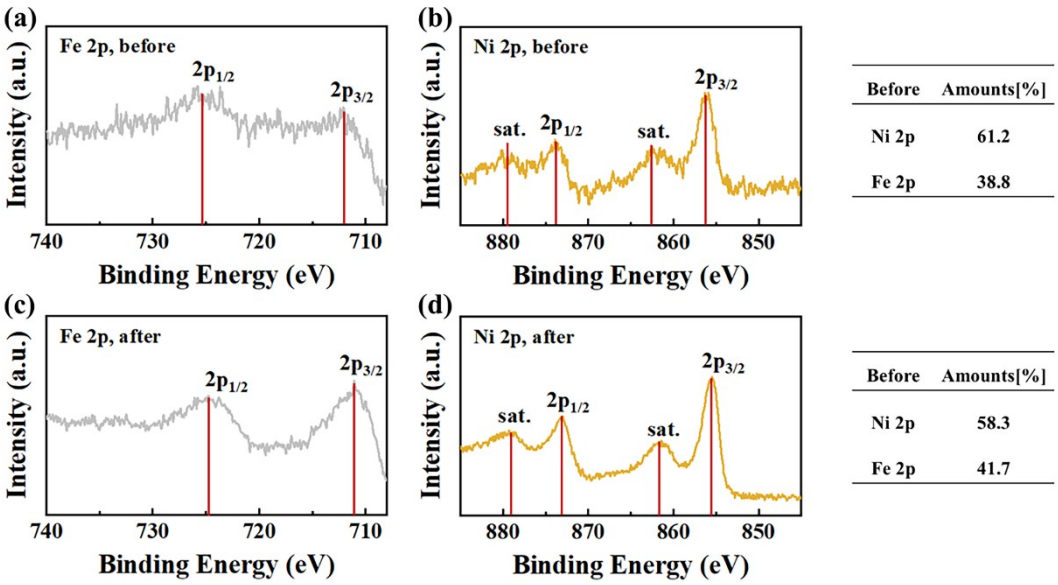

Before	Amounts[%]
Ni 2p	61.2
Fe 2p	38.8

Before	Amounts[%]
Ni 2p	58.3
Fe 2p	41.7

Fig. S7. XPS characterization of the InN/PM6/NiFe LDH photoelectrode before and after the PEC test and changes in Ni and Fe amounts. (a), (c) Fe 2p and (b), (d) Ni 2p XPS spectrum of the InN/PM6/NiFe LDH before and after the PEC test.

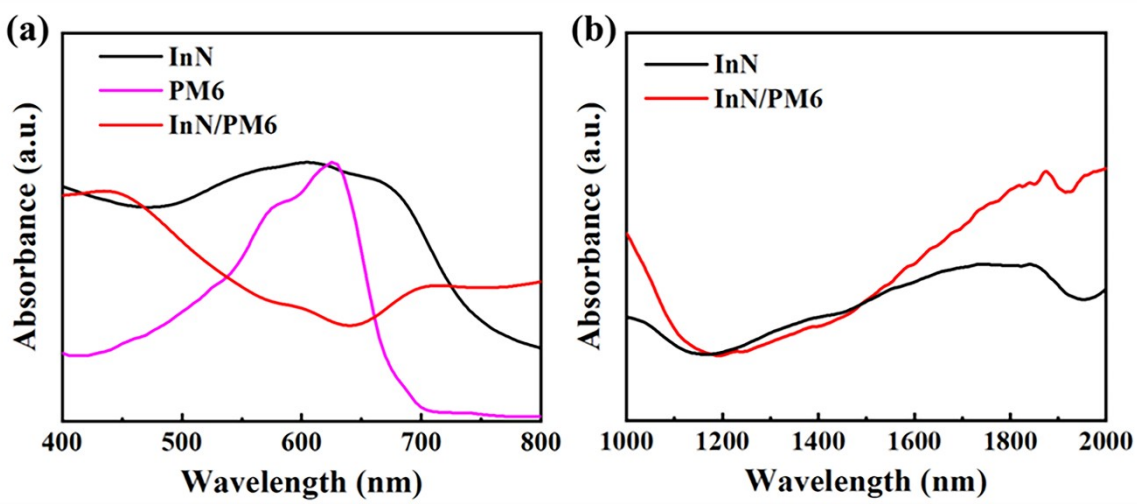

Fig. S8. (a) UV-vis absorption spectroscopy of bare InN NRs, PM6, and InN/PM6 in the visible light region, (b) bare InN NRs and InN/PM6 in the infrared region.

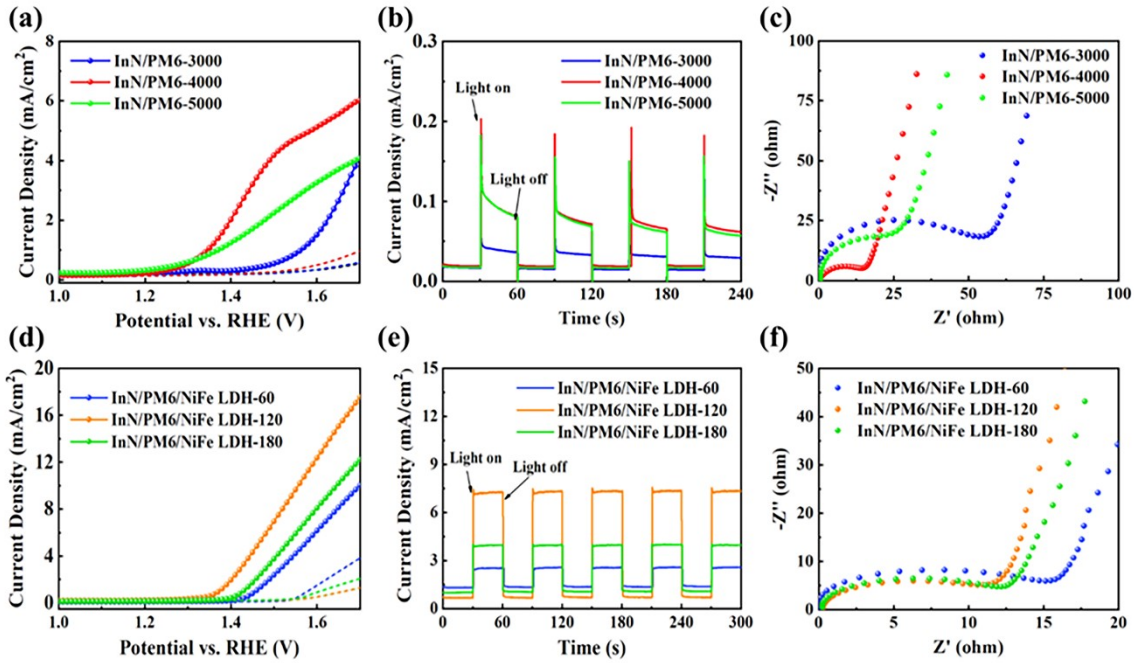

Fig. S9. PEC properties of InN-based photoanode. LSV curves of (a) the InN/PM6 and (d) InN/PM6/NiFe LDH photoanode in 0.1 M KOH solution (pH 13) under 1 sun illumination, Transient photocurrent curves of (b) the InN/PM6 and (e) InN/PM6/NiFe LDH photoanode at 1.45 V vs. RHE, EIS spectra of (c) the InN/PM6 and (f) InN/PM6/NiFe LDH photoanode at 1.2 V vs. RHE.

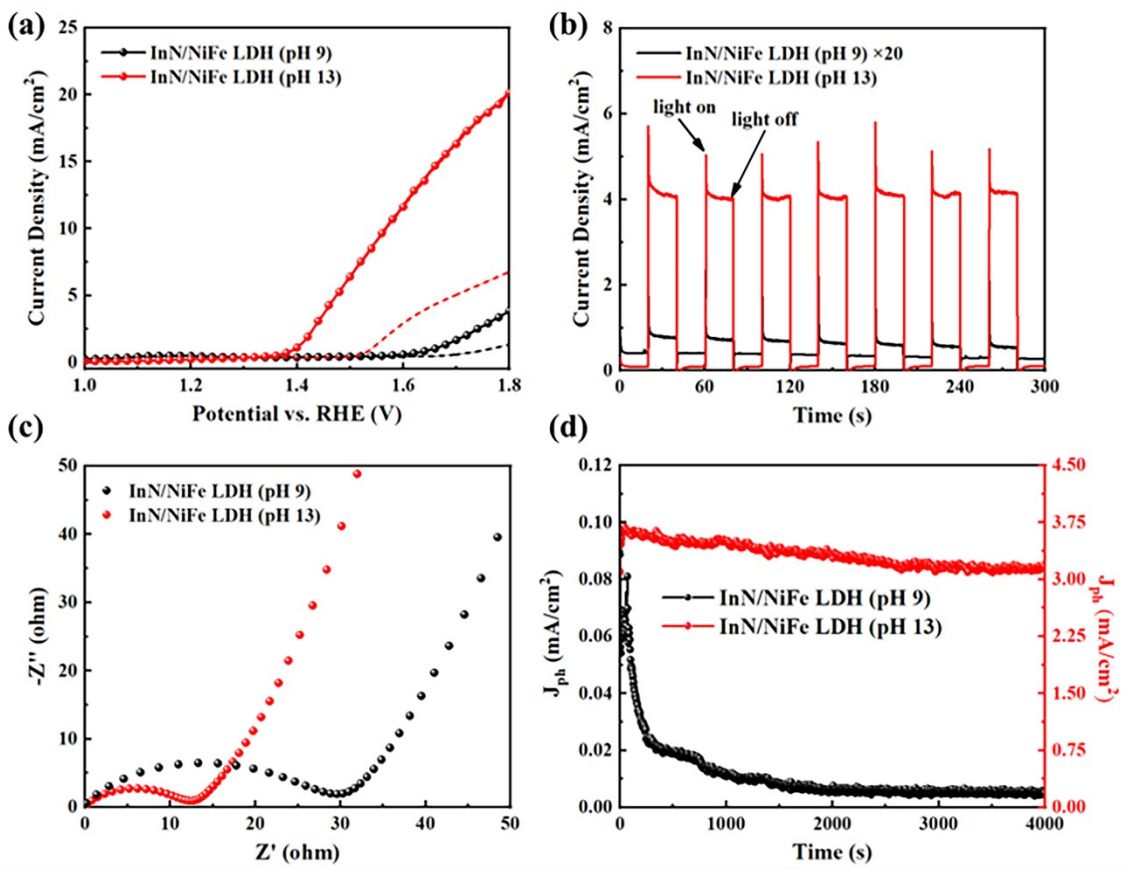

Fig. S10. (a) LSV curves of the InN/NiFe LDH photoanode in 0.2 M Na_2HPO_4 solution (pH 9) and 0.1 M KOH solution (pH 13) under 1 sun illumination. (b)Transient photocurrent curves of the InN/NiFe LDH photoanode at 1.45 V vs. RHE, (c) EIS spectra of the InN/NiFe LDH photoanode at 1.2 V vs. RHE, (d) the J-t curves of the InN/NiFe LDH photoanode in the different pH value of electrolytes at 1.45 V vs. RHE.

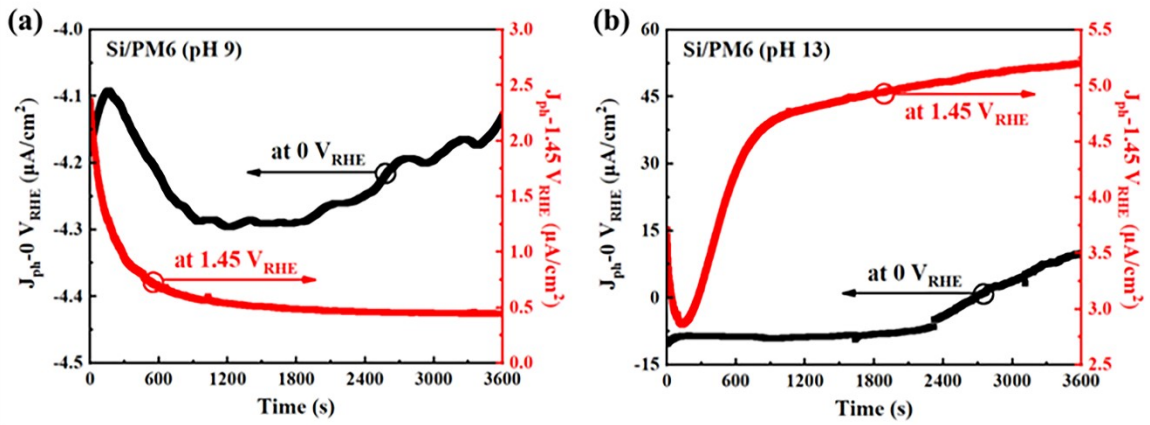

Fig. S11. J-t curves of Si/PM6 photoanodes at 0 V vs. RHE and 1.45 V vs. RHE under 1 sun illumination in 0.2 M Na_2HPO_4 solution (pH 9) and 0.1 M KOH solution (pH 13).

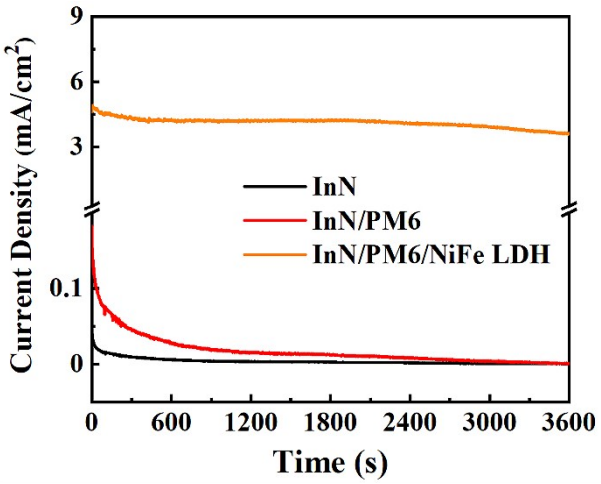

Fig. S12. J-t curves of InN-based photoanodes at 1.45 V vs. RHE under 1 sun illumination in 0.1 M KOH solution (pH 13).

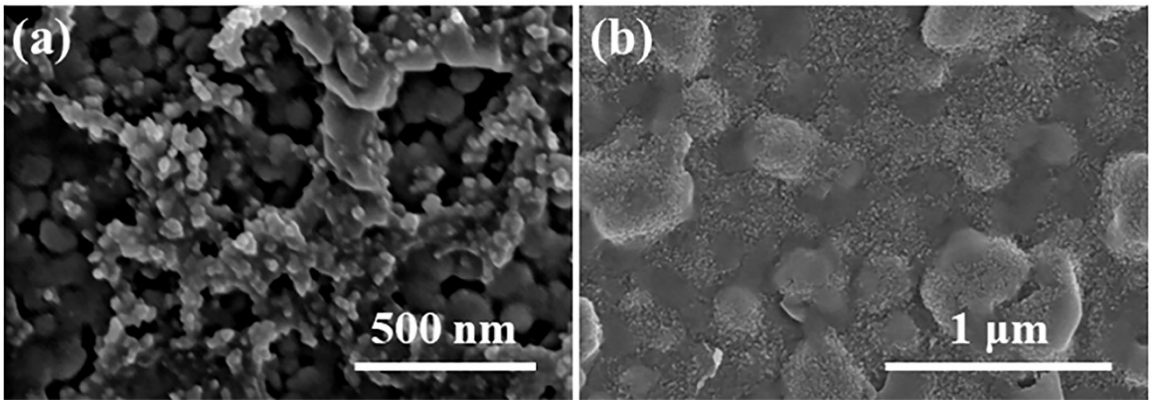

Fig. S13. SEM image of (a) InN/PM6 and (b) InN/PM6/NiFe LDH photoanode after illumination under three-electrodes system.

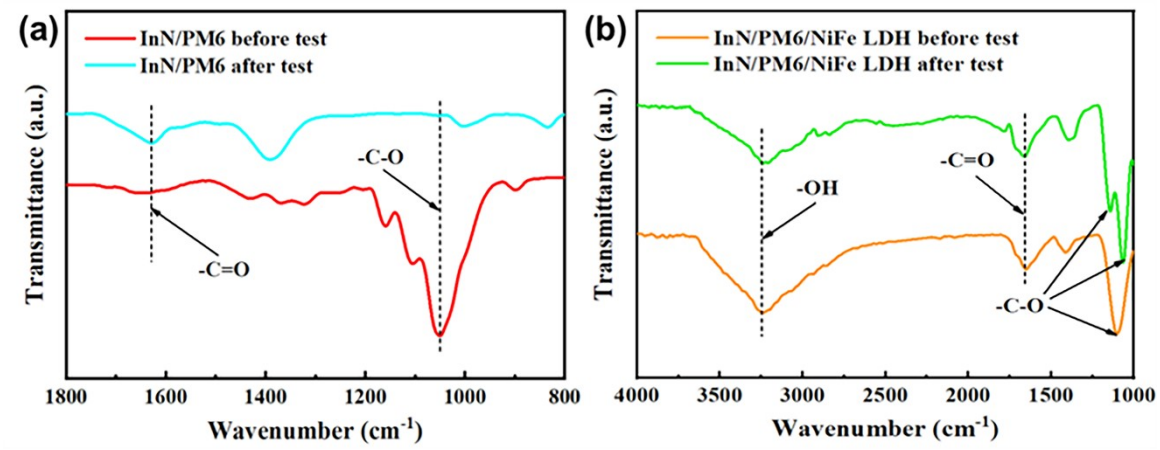

Fig. S14. FT-IR spectrum of (a) InN/PM6 and (b) InN/PM6/NiFe LDH photoanode before and after PEC testing.

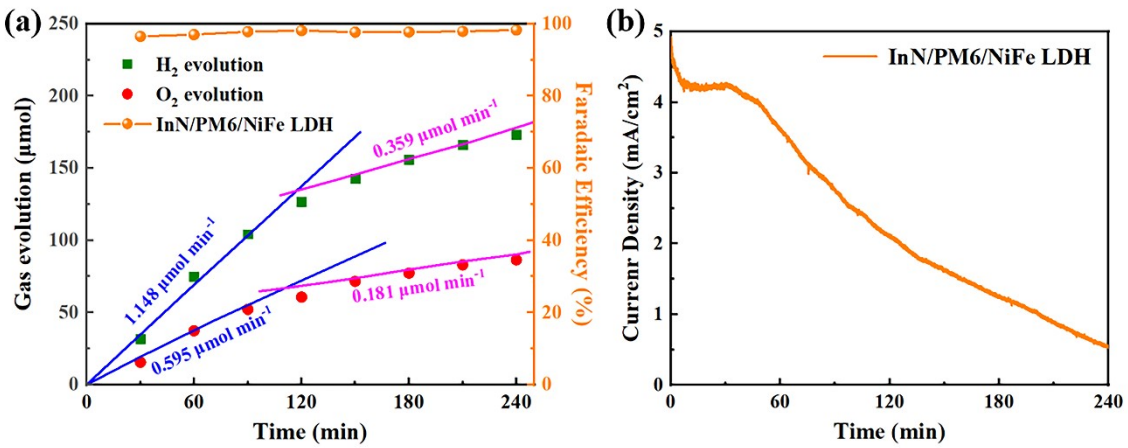

Fig. S15. (a) Gas evolution curves and faradaic efficiency measured under AM 1.5G continuous illumination (b) J-t curves of InN/PM6/NiFe LDH photoanode at 1.45 V vs. RHE under 1 sun illumination in 0.1 M KOH solution (pH 13) for 4 h.

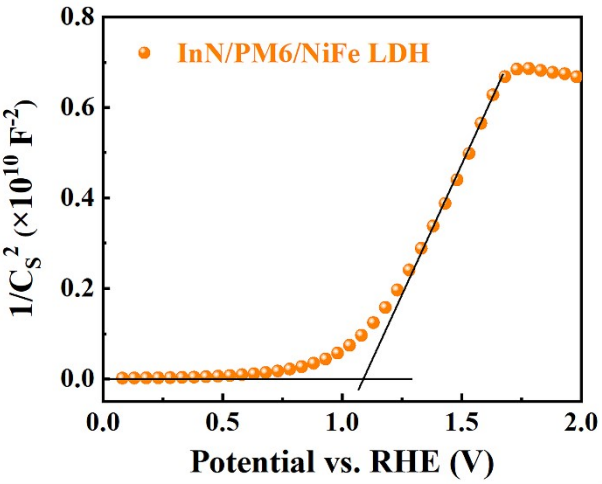

Fig. S16. M-S plots of the InN/PM6/NiFe LDH heterojunction measured in the dark.

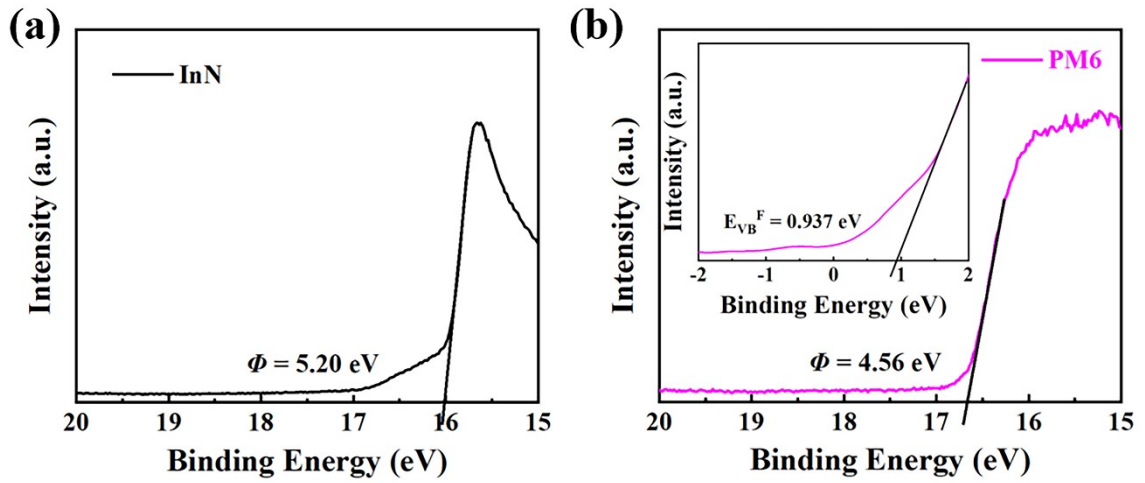

Fig. S17. UPS spectra of (a) InN and (b) PM6. The inset is the corresponding E_{VB}^{F} of PM6.

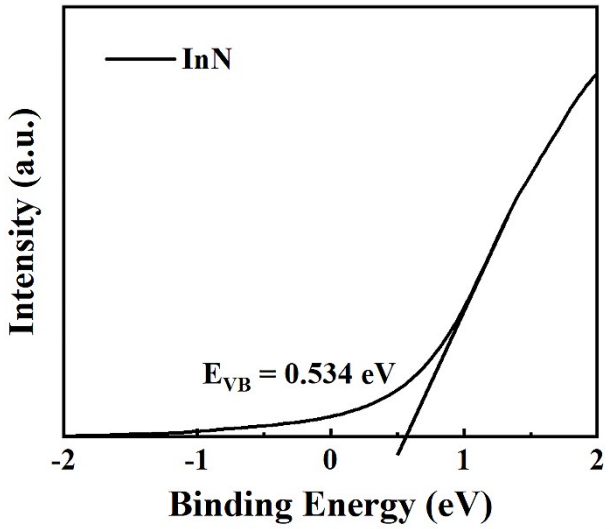

Fig. S18. XPS valence band spectra of the bare InN NRs.

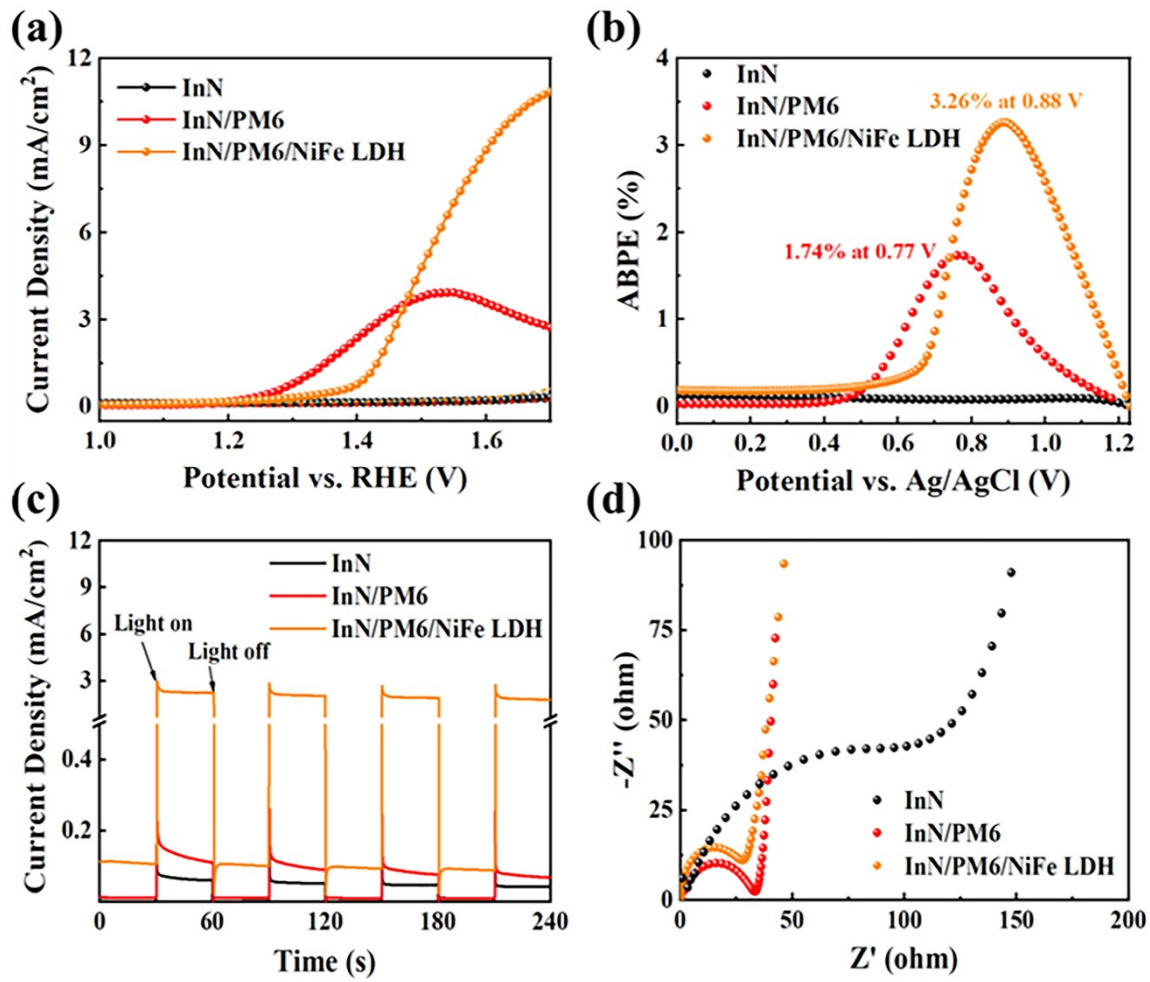

Fig. S19. PEC properties of InN-based photoanode. (a) LSV curves and (b) ABPE curves of the pristine InN NRs, InN/PM6, and InN/PM6/NiFe LDH photoanodes in 0.2 M Na_2HPO_4 solution (pH 9) under 1 sun illumination, (c) Transient photocurrent curves of the different photoanodes at 1.45 V vs. RHE, (d) EIS spectra of all photoanodes at 1.2 V vs. RHE.

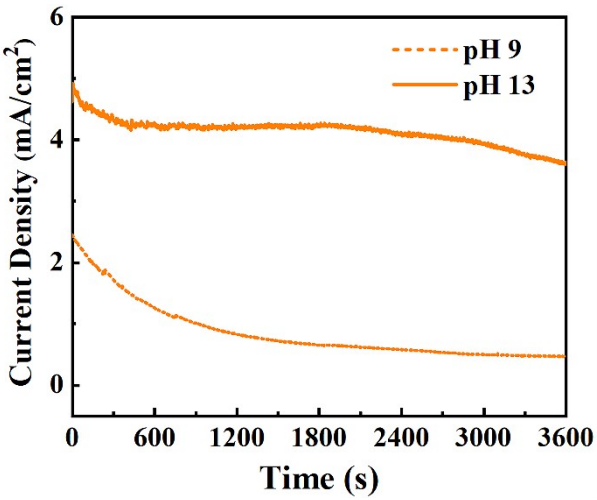

Fig. S20. Chronoamperometry curves of the InN/PM6/NiFe LDH photoanode at 1.45 V vs. RHE under 1 sun illumination in 0.2 M Na_2HPO_4 solution (pH 9) and 0.1 M KOH solution (pH 13).

Table 1. Summary of the PEC performance of InN-based photoanodes under illumination of 100 mW cm^{-2} with AM 1.5G filter.

Photoanode	Electrolyte	Photocurrent density	Reference
InN NRs/PM6	**0.1 M KOH**	**3.21 mA cm^{-2} at 1.45 V_{RHE}**	**This work**
InN NRs/PM6/NiFe LDH	**0.1 M KOH**	**4.82 mA cm^{-2} at 1.45 V_{RHE}**	**This work**
InN NRs/NiFe LDH	**0.1 M KOH**	**3.64 mA cm^{-2} at 1.45 V_{RHE}**	**This work**
InN NW/Si	**1 M NaOH**	**0.06 mA cm^{-2} at 1.2 V_{RHE}**	**Ref. [1]**
In_2O_3/InN	**0.1 M PBS**	**0.795 mA cm^{-2} at 1 $V_{Ag/AgCl}$**	**Ref. [2]**
In_2O_3/InN	**0.1 M PBS**	**0.966 mA cm^{-2} at 1 $V_{Ag/AgCl}$**	**Ref. [3]**
InN/ZnO	**0.1 M Na_2SO_4**	**0.02 mA cm^{-2} at 1.4 V_{RHE}**	**Ref. [4]**
ZnO: InN	**0.5 M Na_2SO_4**	**0.015 mA cm^{-2} at 1 $V_{Ag/AgCl}$**	**Ref. [5]**
Al-rich InAlN	**0.1 M PBS**	**1.2 mA cm^{-2} at 1 $V_{Ag/AgCl}$**	**Ref. [6]**

Table S2. The energy band parameters of all photoelectrodes obtained from the UPS and XPS valence band spectra.

Photoelectrodes	E_{VBM}/E_{HOMO} (eV)	E_{CBM}/E_{LUMO} (eV)	Eg (eV)
InN NRs	**-5.734**	**-5.094**	**0.64**
PM6	**-5.497**	**-3.677**	**1.82**

References

1 J. Kamimura, P. Bogdanoff, M. Ramsteiner, L. Geelhaar and H. Riechert, *Semicond. Sci. Technol.*, 2016, **31**, 6.

2 A. Saroni, S. A. Rahman and B. T. Goh, *7th Asian Conference on Colloid and Interface Science (ACCIS)*, 2017, **5**, S186-S190.

3 A. Saroni, M. Alizadeh, S. A. Rahman, W. Meevasana and B. T. Goh, *J. Power Sources*, 2020, **480**, 10.

4 H. Q. Liu, X. Z. Ma, Z. X. Chen, Q. G. Li, Z. Y. Lin, H. Liu, L. Y. Zhao and S. Chu, *Small*, 2018, **14**, 9.

5 S. S. Menon, H. Y. Hafeez, B. Gupta, K. Baskar, G. Bhalerao, S. Hussain, B. Neppolian and S. Singh, *Renewable Energy*, 2019, **141**, 760-769.

6 M. Alizadeh, G. B. Tong, M. S. Mehmood, K. W. Qader, S. A. Rahman and B. Shokri, *Sol. Energy Mater. Sol. Cells*, 2018, **185**, 445-455.